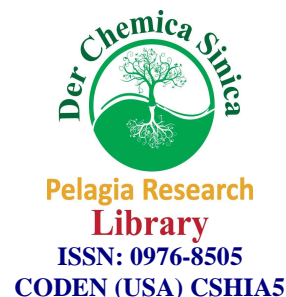




Pelagia Research Library

Der Chemica Sinica, 2012, 3(4):906-913



Growth and characterization of novel (Ni^{3+} , Mg^{2+}) bimetallic crystals of ammonium di hydrogen phosphate

A. Claude

Post Graduate and Research Department of Physics, Government Arts College, Dharmapuri,
Tamil Nadu, INDIA

ABSTRACT

Ammonium Di-hydrogen Phosphate (ADP), crystals are good Second Harmonic Generators (SHG) having appreciable Non Linear Optic (NLO) properties. These ADP crystals when mixed with metallic radicals show a visible modification in the change of growth habit during growth. Bimetallic crystal Nickel Magnesium (Ni^{3+} , Mg^{2+}) Ammonium Di-hydrogen Phosphate (NMADP), when analysed for structural and optical characteristics show a visible change in their properties, compared to the pure crystal of ADP. FTIR investigations reveal that the inclusion of the metallic impurities extend the transmission region to a great extent, where the HRXRD reveals that the crystallinity of the material is superior in the pure form than the bimetallic form conforming the inclusion of the bimetals. The conversion efficiency and SHG generation of the grown crystals were also confirmed.

KEYWORDS: Crystal Growth, ADP, Nonlinear Materials, Second Harmonic Generator, HXRD, properties

INTRODUCTION

Ammonium di-hydrogen Phosphate (ADP) is a well known NLO material which also has many interesting Ferroelectric and Anti-ferroelectric properties. ADP was one among the earliest materials which were exploited for their NLO properties. They are still widely used as non linear optic devices and are the choicest electro-optic materials having wide practical applications [1-5]. Presence of small amount of impurities in the form of anionic bimetallic dopants Ni^{3+} , Mg^{2+} plays a vital role in the growth rate, habit of the crystal and its properties. The inclusion of these dopants added in the optimal stiochiometric ratio can possibly play a significant part in altering the properties of the parent crystal. Crystals of ADP were grown by solution growth technique by slow evaporation technique at room temperature. Bimetallic dopants were added in the optimal stiochiometric ratio.

MATERIALS AND METHODS

CRYSTAL GROWTH

Crystal growth of pure and bimetallic ADP was done by solution growth technique at room temperature. The solubility [6] of ADP in the pure state and that of ADP with Nickel and Magnesium were studied. It was observed that solubility of ADP in its undoped state was found to be 32 g per 100 mL of the solvent (double distilled water). By adding Nickel and Magnesium (Ni^{3+} , Mg^{2+}) it was observed that the solubility decreased by 30g which is attributed to the impurities that were added.

The metastable zone width [7,8] measures the stability of a solution in its supersaturated region where the largest width implies the substance having higher growth stability. 100 mL of the saturated solution was kept in the cryostat and the temperature reduced at 5°C h^{-1} while the solution was stirred continuously. The temperature of formation of the first speck was found. The metastable zone width of ADP was found to be the maximum in the lower temperature gradients than the higher gradients. With the addition of the bimetallic impurities it was further noted that the metastable zone decreased marginally due to the presence of dopants. But no spontaneous nucleation was observed which explains the stability of the solution until complete crystal growth.

CHARACTERIZATION

X-Ray Diffraction studies were carried out with the grown crystals in powdered form. The powder samples were loaded into a Rigaku X-Ray diffraction apparatus using $\text{CuK}\alpha$ radiation having $\lambda = 1.5405$ and analysed. Results were compared with the JCPDS database file number 37-1479 where the prominent peaks of the reported values coincided with the investigated patterns. The powder XRD pattern of ADP (Fig. 1) as well as bimetallic Nickel-Magnesium (Ni^{3+} , Mg^{2+}) ADP (Fig. 2) had three common prominent peaks at (202), (201), (204) respectively. Another prominent peak with maximum intensity was observed at (101) for the (Ni, Mg) ADP bimetallic crystal which can be due to the presence of the bonding signature between (Ni, Mg) bimetals and ADP. The cell parameters were found to be $a = 7.502 \text{ \AA}$, $c = 7.554 \text{ \AA}$ respectively. The cell volume was found to be 425.139 \AA^3 .

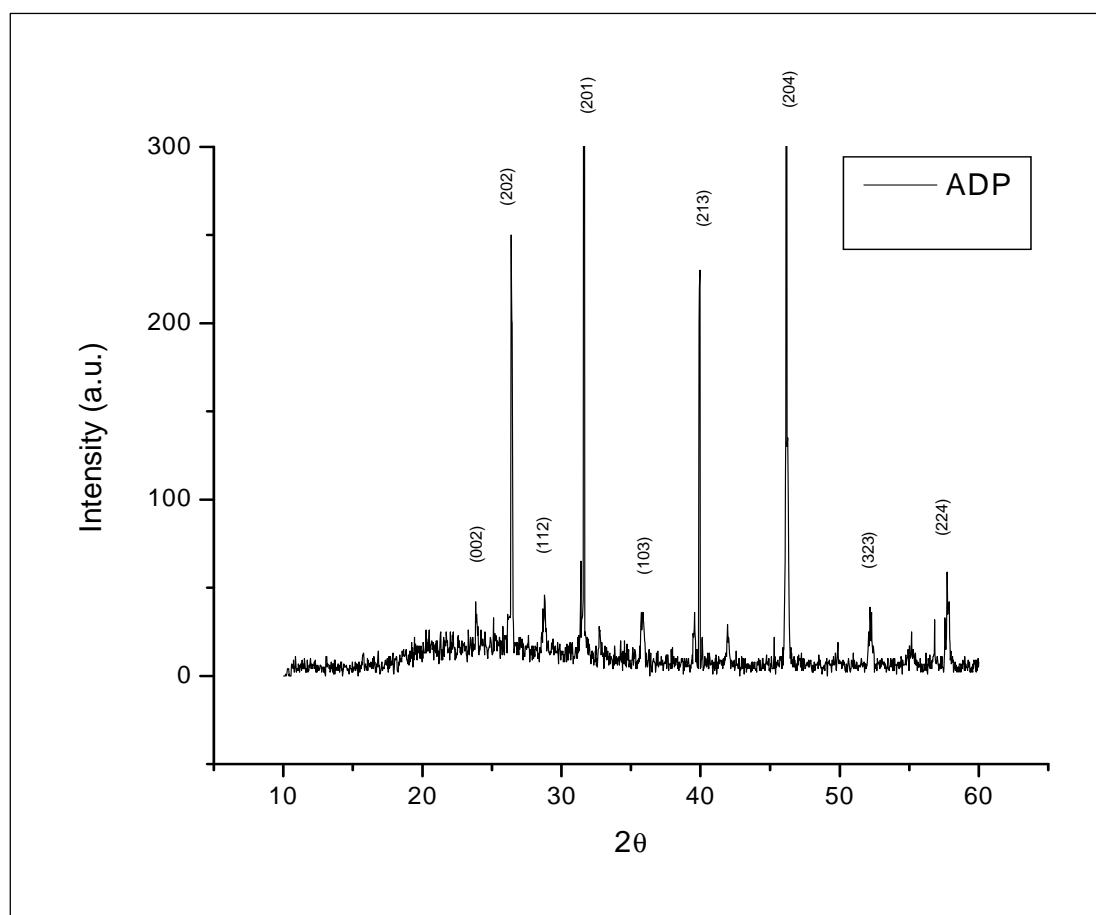


Fig. 1: Powder XRD of pure ADP crystal

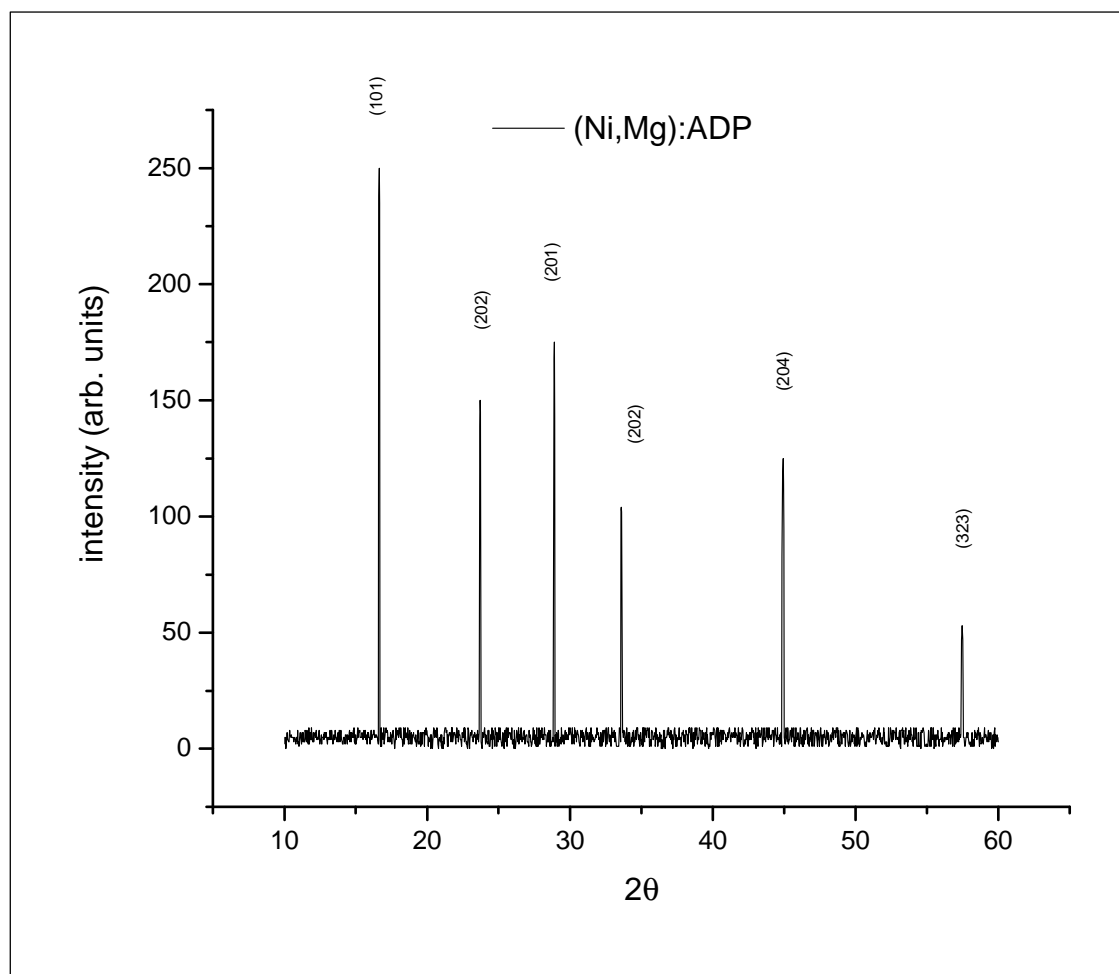


Fig. 2: Powder XRD of (Ni-Mg) ADP

FTIR INVESTIGATIONS

Infrared spectrometry [9] involves examination of the twisting, bending, rotating and vibrational modes of atoms in a molecule. Upon interaction with infrared radiation, portions of the incident radiation are absorbed at specific wavelengths. The multiplicity of vibrations occurring simultaneously produces a highly complex absorption spectrum that is uniquely characteristic of the functional groups that make up the molecule and of the overall configuration of the molecule as well.

The Fourier Transform Infra Red (FTIR) investigations were also carried out on the powdered samples of ADP and bimetallic ADP. The spectrum was observed from a Perkin-Elmer 781 spectrophotometer in the regions 400 to 4000 cm^{-1} using a KBr pellet. Many useful observations were observed. The group frequency region was located between (4000 to 1300 cm^{-1}) and the fingerprint region (1300 to 650 cm^{-1}). The intermediate frequency range, 2500 to 1540 cm^{-1} (*unsaturated* region) contains triple bond frequencies which appear from 2500 to 2000 cm^{-1} and double bond frequencies from 2000 to 1540 cm^{-1} . In the region between 1300 and 650 cm^{-1} there are single bond stretching frequencies and bending vibrations (skeletal frequencies) of polyatomic systems involving motions of bonds linking a substituent group to the molecule. The lower regions 667 to 10 cm^{-1} contains the bending vibrations of carbon, nitrogen, oxygen and fluorine with atoms heavier than mass 19. The observed frequencies for the diatomic molecule O_2 was at 1582 cm^{-1} . Dopants like Mg had absorption peaks (Fig.3,4) at 621 cm^{-1} , Ni^{3+} at 540 cm^{-1} and strong absorption bands for lattice water (antisymmetric and symmetric OH stretchings) at 3231 cm^{-1} were also observed. This can be attributed to the fact, that when certain solutes crystallize from aqueous solutions, they are the hydrated salts, which contain water and solute in a specific stoichiometric ratio. The water in such instances is referred to as

water of hydration, and the number of water molecules associated with each solute molecule may vary with the crystallization temperature. It was observed (Fig.5) in Ni^{3+} doped ADP an additional absorbance was detected at 3237 cm^{-1} which implies that the inclusion of Nickel modifies the transparency of the crystal at that region. Nickel Magnesium bimetallic ADP crystal had an increased absorbance at 3293 cm^{-1} , the peak at 2242 cm^{-1} is found to be missing and the peak at 3325 cm^{-1} seems to broaden up. This can be attributed to the double dopant introduced.

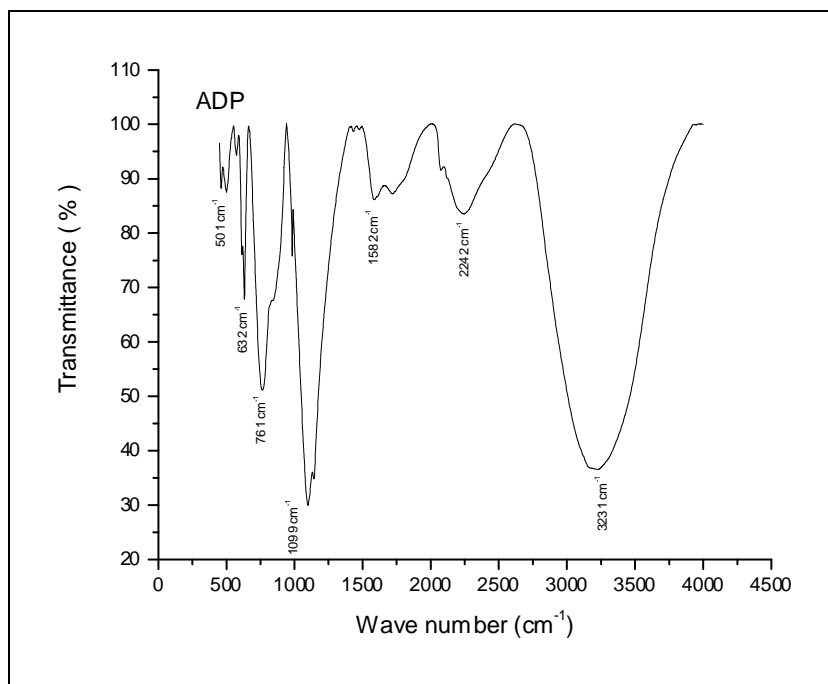


Fig.3: FTIR spectrum of pure ADP crystal

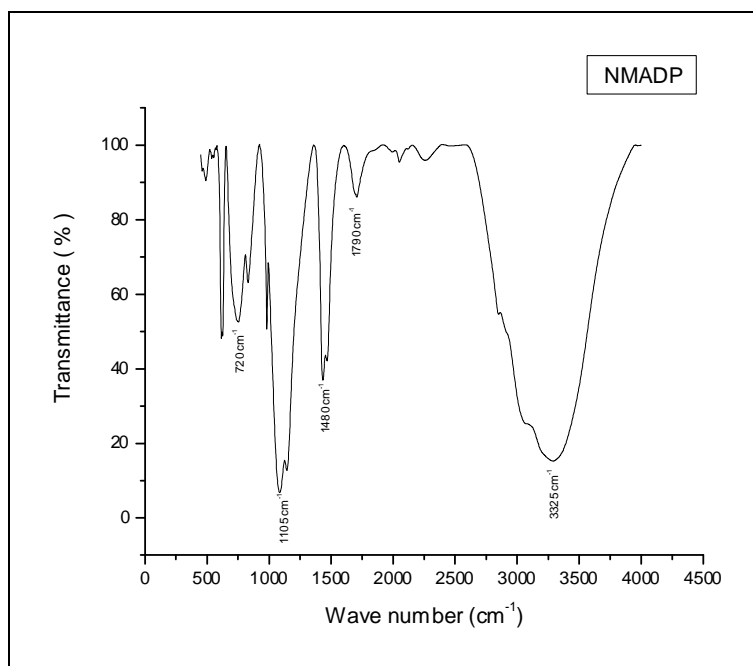


Fig. 4: FTIR spectrum of (Ni-Mg) ADP crystal

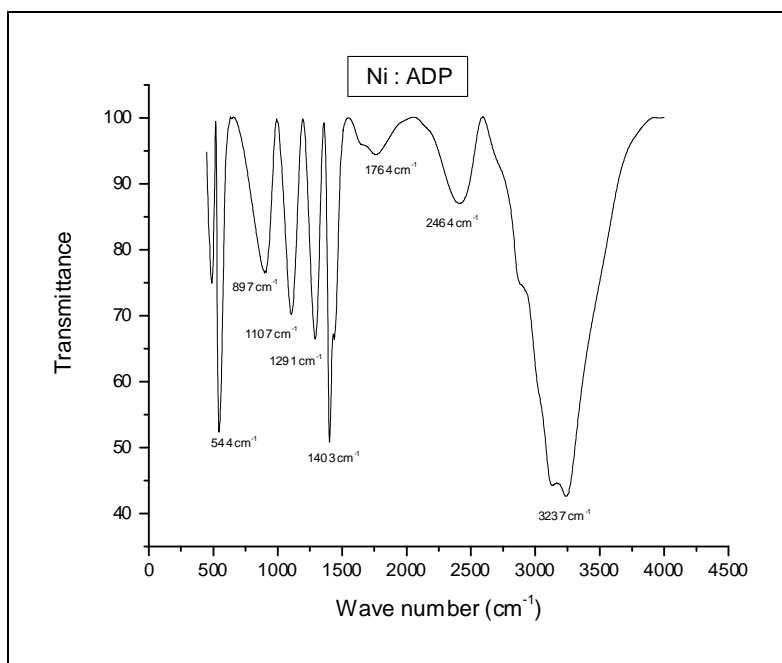


Fig. 5: FTIR spectrum of Ni: ADP crystal

MICROHARDNESS MEASUREMENTS

Microhardness tests are useful to find the mechanical hardness of the crystal grown and to estimate the threshold mechanical stress it can withstand. Samples of pure ADP and bimetallic Nickel-Magnesium ADP were indented using a Lietz-Wetzler P1191 Microhardness tester fitted with a Vickers pyramidal indenter having an optical angle of 136° between the opposite pyramids. Observations of the various indentation tests were done using the Metallux-II Metallurgical Microscope.

An indentation time of 10 s were applied uniformly for loads 20 to 90 g. The hardness value of the cut and polished Lithium Niobate crystal samples (Fig.6) were found to decrease slowly with the applied loads until 40 g. Further application of higher loads showed that the hardness values sharply decreased and developed mild cracks on the pyramidal indentation edges. Beyond 90 g the samples developed large prominent cracks due to the attainment of the threshold mechanical stress. The hardness values were calculated using the formula

$$H_v = \frac{1.8544 \times P}{D^2} \text{ kg mm}^{-2}$$

H_v is the Vickers hardness number. P is the indenter load in gm and D is the diagonal length of the impression in mm. The micro hardness value was taken as the average of the several impressions made with both diagonals being measured.

In the present study, the hardness of the pure ADP is higher than that of bimetallic Nickel Magnesium ADP added KDP crystal. This is because of the incorporation of the Nickel and Magnesium (Ni^{3+} , Mg^{2+}) ions into superficial crystal lattice and forming defect centers which generate weak lattice stresses on the surface.

UV-VIS-NIR SPECTRAL ANALYSIS

The UV-Vis-NIR spectral transmittance was studied using a Shimadzu UV-1061 UV-Vis spectrophotometer with a single crystal of 2 mm thickness in the range of 200-1200 nm. The crystal has sufficient transmission in the entire visible and IR region. The lower cut off wavelength is around 350 nm; the transmission percentage of Nickel and Magnesium (Ni^{3+} , Mg^{2+}) added ADP crystal is around 65%, as compared to pure KDP, which is around 55%. (Fig. 7)

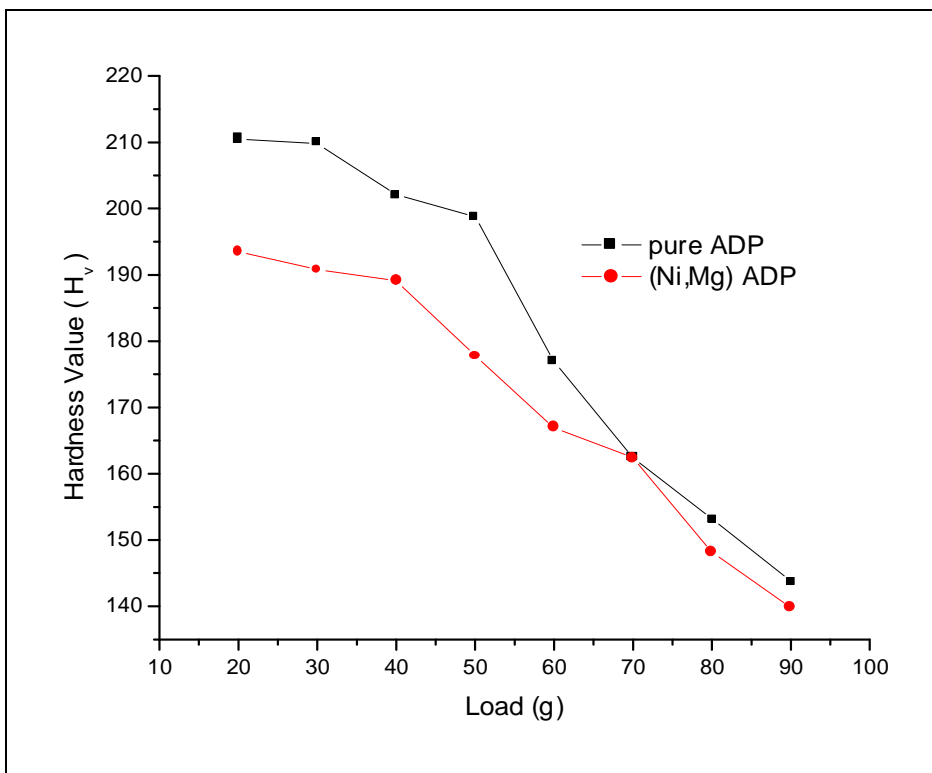
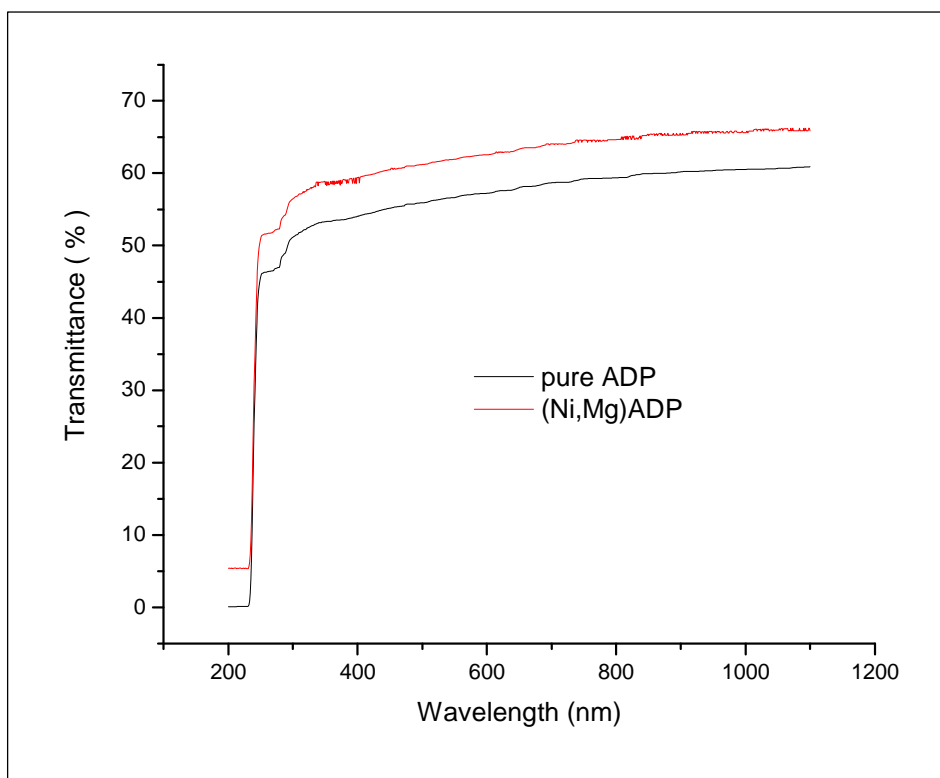


Fig. 6: Microhardness curve of pure and bimetallic ADP

Fig. 7: UV-Vis-NIR spectra of ADP and bimetallic ADP



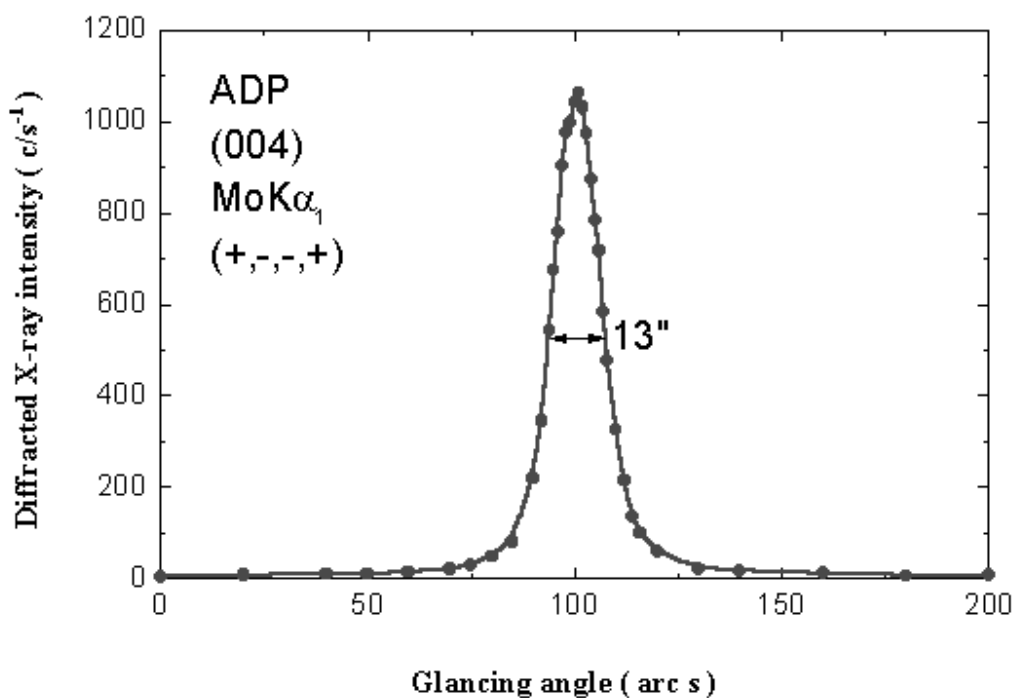


Fig 8: HRXRD of pure ADP crystal

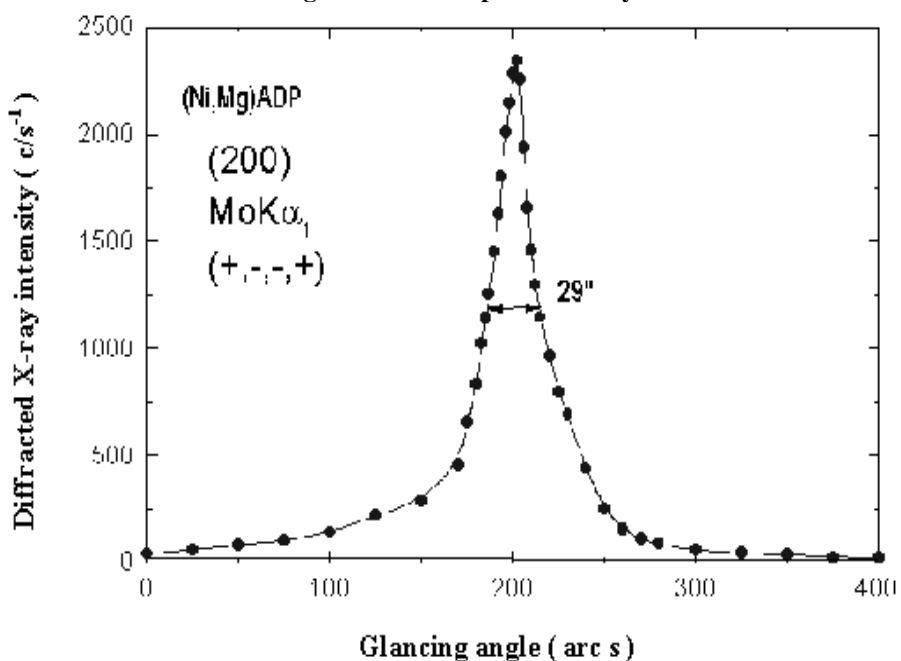


Fig. 9: HRXRD of (Ni, Mg)ADP crystal

HIGH RESOLUTION XRD ANALYSIS

The high-resolution diffraction curves recorded for specific diffracting planes which are mentioned in the curved brackets with the multicrystal X-ray diffractometer [10] in symmetrical Bragg geometry. A well-collimated and monochromated MoK α_1 beam obtained from a set of three plane (111) Si monochromator crystals set in dispersive (+,-,-) configuration has been used as the exploring X-ray beam. The specimen crystal is aligned in the (+,-,-,+) configuration. Due to dispersive configuration, though the lattice constant of the monochromator crystal(s) and the

specimen are different, the unwanted dispersion broadening in the diffraction curve of the specimen crystal is insignificant.

Both the curves were observed to have single peaks. This diffraction curve (Fig. 7) shows that though the quality of this crystal is very good, the specimen contains one *very low* angle boundary. The FWHM of the ADP peaks (Fig. 8) were 13'' and the Nickel-Magnesium (Ni^{3+} , Mg^{2+}) ADP crystal (Fig. 9) was 29''. This implies that the pure crystal of ADP had a higher order of crystallinity than the Nickel and Magnesium bimetallic (Ni^{3+} , Mg^{2+}) ADP crystal.

CONVERSION EFFICIENCY

The conversion efficiency of the crystal was checked using the powder SHG technique developed by Kurtz and Perry[11]. The crystal was ground into powder and densely packed in between two glass slides. An Nd:YAG laser beam of wavelength 1064 nm was made to fall normally on the sample cell. The emission of green light confirms the second harmonic generation on ADP as well as Nickel Magnesium ADP crystals.

CONCLUSION

Crystals of Bimetallic (Ni^{3+} , Mg^{2+})ADP were grown by low temperature solution growth technique at room temperature. The change in structural, optical and qualitative properties were analysed in comparison with pure ADP crystal [12-14]. It was found that NLO grade bimetallic crystals of ADP showed low crystallinity than the pure KDP crystals. The transparency of the newly harvested bimetallic crystal of KDP was observed to be more than the pure crystal of KDP [15-16]. Crystals of ADP grown using bimetallic dopants were found to be stronger than pure crystals.

Acknowledgements

The author A.C wish to thank Dr. R. Gopalakrishnan and Prof. P. Ramasamy, former Director, Crystal Growth Centre, Anna University, presently Dean (Research), SSNCE, Kalavaakam for fruitful suggestions, Dr. N. Vijayan and Dr. G. Bagavannarayana of National Physical Laboratory, New Delhi and Dr. V. Vaithianathan, China for extending many characterization facilities. The author also wishes to thank Dr. P. K. Baskaran, Principal (i/c) and Prof. A. Poyyamozhi, Head, PG and Research Department of Physics for their encouragement and support.

REFERENCES

- [1] A.M.Glass and M.E. Lines, *Principles and Applications of Ferroelectric and Related Materials*, Oxford University Press, Oxford, **1977**, p293.
- [2] E. Courtens, *Helv. Phys. Acta.*, **1983**, 56:705.
- [3] D. Ermerl, *Ferroelectrics*, **1987**, 72: 95.
- [4] N.P. Zaitseva, L.N.Rashkovich and S.V.Bogatyreva, *J. Crystal Growth*, **1995**, 148:276.
- [5] Dmitriev V.G, Gurzadyan G.G, Nikogosyan D.N, *Handbook of Nonlinear optical crystals*, Springer-Verlag, Berlin, Heidelberg, **1991**, pp14-35.
- [6] Chernov A.A, *Modern Crystallography-III – Crystal Growth*, Springer Verlag, Solid State Series 36, New York, **1984**, pp100-251.
- [7] Zaitseva N.P, L.N.Rashkovich and S. V. Bogatyreva, *J. Crystal Growth*, **1995**, 148: 276.
- [8] J Zachova, J.Shtepanek and N.P.Zaitseva, SPIE, USSR-CSFR Joint seminar on Nonlinear Optics in Control, Diagnostics and Modelling of Biophysical Process, **1990**, 1402: 225-250.
- [9] Petinari C Ed, *Vibrational Rotational and Raman Spectroscopies*, Academic Press, Singapore, **1999**, pp1021-1032.
- [10] Lal K and G. Bhagavannarayana, *J. Crystal Growth*, **1989**, 22: 209-215
- [11] Kurtz S.K and Perry T.T, *J. Applied Phys*, **1968**, 39: 3798.
- [12] D. K. Sawant and D. S. Bhavsar, *Der Chemica Sinica*, **2011**, 2 (4): 211-218.
- [13] S. K. Yadav, A. N. Thakur, A. Kumar, S. N. Singh, K. C. Mourya and V. P. Srivastava, *Der Chemica Sinica*, **2011**, 2 (1): 149-156.
- [14] N. S. Shinde, S. S. Khot, B. P. Ladgaonkar, B. B. Kale, S. Apte, P. M. Tamhankar and S. C. Watawe, *Der Chemica Sinica*, **2011**, 2 (4):252-261.
- [15] Sachin. V. Bangale, S. M. Khetre and S. R. Bamane, *Der Chemica Sinica*, **2011**, 2 (4):303-311.
- [16] Pushkar P. Kalantri, Rakesh R. Somani and Dinesh T. Makhija, *Der Chemica Sinica*, **2010**, 1 (1): 1-12.